

E1-2009-187

V. P. Ladygin\*, A. P. Jerusalimov, N. B. Ladygina

POLARIZATION OF  $\Lambda^0$  HYPERONS  
IN NUCLEUS–NUCLEUS COLLISIONS  
AT HIGH ENERGIES

Submitted to «Письма в ЭЧАЯ»

---

\*E-mail: vladygin@jinr.ru

Ладыгин В. П., Иерусалимов А. П., Ладыгина Н. Б. Е1-2009-187  
Поляризация  $\Lambda^0$ -гиперонов в ядро-ядерных столкновениях при высоких энергиях

В качестве одного из возможных способов изучения фазового перехода рассматривается измерение поляризации  $\Lambda^0$ -гиперонов в ядро-ядерных столкновениях. Обсуждаются эксперименты на фиксированной мишени и коллайдере для случая рождения  $\Lambda^0$ -частиц в центральных Au–Au-столкновениях при  $\sqrt{s_{NN}}$  порядка нескольких ГэВ.

Работа выполнена в Лаборатории физики высоких энергий им. В. И. Векслера и А. М. Балдина ОИЯИ.

Препринт Объединенного института ядерных исследований. Дубна, 2009

Ladygin V. P., Jerusalimov A. P., Ladygina N. B. E1-2009-187  
Polarization of  $\Lambda^0$  Hyperons in Nucleus–Nucleus Collisions at High Energies

The measurement of  $\Lambda^0$ -hyperon polarization in nucleus–nucleus collisions is considered as one of possible tools to study the phase transition. Fixed target and collider experiments are discussed for the case of  $\Lambda^0$  production from Au–Au central collisions at  $\sqrt{s_{NN}}$  of about several GeV.

The investigation has been performed at the Veksler and Baldin Laboratory of High Energy Physics, JINR.

Preprint of the Joint Institute for Nuclear Research. Dubna, 2009

## INTRODUCTION

The phase transition from ordinary nuclear matter to a quark–gluon plasma (QGP) should be observed when conditions of sufficiently high baryonic densities and/or temperatures are achieved during the heavy-ion collisions. There is a number of experimental observables to identify this transition, such as strangeness enhancement, charmonium suppression, event anisotropy, fluctuation in particles ratios, transverse momenta, etc. At the same time, it has also been recognized that no single signal alone can provide clear evidence for the existence of the phase transition. This stimulates the search for new probes to investigate the properties of hot and dense matter produced in heavy-ion collisions at high energies.

One of the new signatures can be the change in the polarization properties of the secondary particles in the nucleus–nucleus collisions compared to the nucleon–nucleon collisions. A number of polarization observables have been proposed as a possible signature of phase transition, namely, decreasing of the  $\Lambda^0$  transverse polarization in central collisions [1, 2], non-zero  $\bar{\Lambda}^0$  longitudinal polarization [3, 4], non-zero  $J/\Psi$  polarization at low  $p_T$  [5], anisotropy in di-electron production from vector mesons decay [6] (and references therein), global hyperon polarization [7] and spin-alignment of vector mesons [8] in non-central events, etc.

The strangeness enhancement is considered as one of the signal of the phase transition from ordinary matter to quark–gluon plasma (QGP). The strong strangeness enhancement at  $\sim 30 \text{ GeV} \cdot A$  as well as the change of the slope of the strange particles spectra have first been observed by the NA49 collaboration in both kaon [9] and hyperon [10] data. In this respect the study of the polarization properties of the hyperons at the energies  $\sqrt{s_{NN}}$  of several GeV is of great interest.

However, in spite of the large amount of the data on the  $\Lambda^0$  production obtained at GSI [11], AGS [12–14], SPS [10] and RHIC [15–19], there are only few results on the  $\Lambda^0$  polarization in nucleus–nucleus interaction [20–23].

The goal of the present paper is to summarize the existing experimental data and to discuss the possibility of the  $\Lambda^0$ -polarization measurements in nucleus–nucleus collisions at  $\sqrt{s_{NN}}$  of several GeV at future setups.

## 1. $\Lambda^0$ POLARIZATION IN PROTON-INDUCED REACTIONS

Since the first observation of large transverse polarization of  $\Lambda^0$  hyperon [24, 25] in inclusive nucleon–nucleon and nucleon–nuclei interactions, there has been permanent interest in the origin of this effect. A significant amount of the data on  $\Lambda^0$  polarization has been accumulated at different nucleon initial energies between 6 and  $\sim 2000$  GeV [26]. All these measurements indicated that the high-energy hyperon polarization is a function only of the hyperon transverse momentum  $p_T$  and the fraction of the beam energy carried by the final-state hyperon  $x_F$ . The magnitude of the polarization at fixed  $x_F$  rises with  $p_T$  to a plateau at about 1 GeV/c, and the size of the plateau increases monotonically with  $x_F$ . A minor dependence of the  $\Lambda$  polarization on the  $A$  value of the target has been observed.

Most of the models explain the  $\Lambda^0$  polarization by the recombination of a polarized  $s$  quark with an unpolarized ( $ud$ ) spectator diquark. In this case the spin of  $\Lambda^0$  is carried by the produced  $s$  quark and that the  $u$  and  $d$  quarks can be thought of as being coupled into a diquark with zero total angular momentum and isospin.

In the framework of the semiclassical recombination model of DeGrand–Miettinen [27] the  $\Lambda^0$  polarization is defined by the slow  $s$ -quark spin precession. According to this model,  $\Lambda^0$  polarization is expressed as follows:

$$\mathcal{P}_{\Lambda^0} = -\frac{12}{\Delta x_0 M^2} \frac{1 - 3\xi(x)}{[1 + 3\xi(x)]^2} p_T, \quad (1)$$

where

$$M^2 = \frac{m_D^2 + p_{TD}^2}{1 - \xi(x)} + \frac{m_s^2 + p_{Ts}^2}{\xi(x)} - m_{\Lambda^0}^2 - p_T^2 \quad (2)$$

with  $m_D, p_{TD}$  ( $m_s, p_{Ts}$ ) the mass and transverse momentum of the  $ud$  diquark ( $s$  quark),  $m_{\Lambda^0}$  and  $p_T$  the mass and transverse momentum of the  $\Lambda^0$ ,  $\Delta x_0$  a distance scale and  $\xi(x) = x_s/x$  the ratio of the longitudinal momentum of the  $s$  quark to the longitudinal momentum fraction of the  $\Lambda^0$  with respect to the beam proton.

The parametrization taken in the form

$$\xi(x) = \frac{1}{3}(1 - x) + 0.1x \quad (3)$$

gives a quantitative description for the  $\Lambda^0$  polarization in nucleon–nucleus interaction within a wide energy range [24–26].

## 2. $\Lambda^0$ POLARIZATION IN HEAVY-ION COLLISIONS

In the case of relativistic nucleus–nucleus collisions, the expectation is that  $\Lambda^0$ 's coming from the region where the critical density for QGP formation has been achieved are produced through the coalescence of independent slow sea  $u$ ,  $d$  and  $s$  quarks. Therefore, the plasma creates  $\Lambda^0$  with zero polarization [2]. Finally, in the case of QGP formation the depolarization effect compared to proton-induced reaction should be observed. The total cross section of  $\Lambda^0$  production versus impact parameter  $b$  is the sum of the cross sections for the peripheral collisions and QGP regions [2]:

$$\frac{d^2\sigma_{\Lambda^0}}{d^2b} = \frac{d^2\sigma_{\Lambda^0}^{\text{per}}}{d^2b} + \frac{d^2\sigma_{\Lambda^0}^{\text{QGP}}}{d^2b}. \quad (4)$$

Since  $\Lambda^0$ 's from QGP zone have a zero polarization, one can write

$$\mathcal{P}_{\Lambda^0} = \frac{\mathcal{P}_{\Lambda^0}^{\text{per}}}{1 + f(b)}, \quad (5)$$

$$f(b) = \frac{d^2\sigma_{\Lambda^0}^{\text{QGP}}}{d^2b} \bigg/ \frac{d^2\sigma_{\Lambda^0}^{\text{per}}}{d^2b}, \quad (6)$$

where  $f(b)$  is defined as the ratio of the differential cross sections for  $\Lambda^0$  production from the QGP and recombination processes.

The behavior of  $f(b)$  as a function of impact parameter  $b$  for RHIC energies is shown in Fig. 1 [2]. One can expect up to 30–40% of the depolarization effect for the central events. It is shown that the measurable depolarization effect can be observed at the  $\Lambda^0$  transverse momenta  $p_T \geq 0.6$ – $0.8$  GeV/ $c$ .

The measurements of  $\Lambda^0$  transverse polarization in nucleus–nucleus collisions [20–22] have shown that the produced  $\Lambda^0$ 's are still polarized at freeze-out that means the spin direction is only little affected by the rescattering phase after hadronization. However, there was no scan versus the centrality in this experiment.

Another novel phenomenon is so-called global polarization [7,8]. System in the noncentral collisions have large orbital angular momentum, which manifests

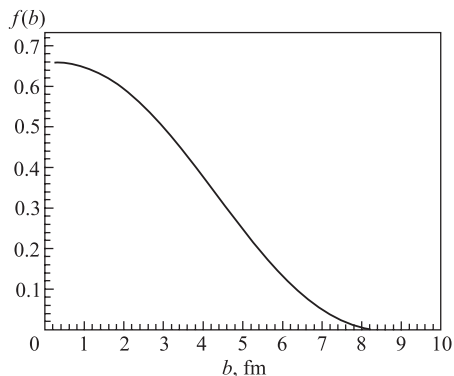


Fig. 1. The ratio of the differential cross sections for  $\Lambda^0$  production from the QGP and recombination processes [2]

itself in the polarization of secondary particles along the direction of the system angular momentum.

Parton interaction in noncentral relativistic nucleus–nucleus collisions leads to the global polarization of the produced quarks. This value for RHIC energies can be about 30% and would lead to the global polarization of hyperons [7]. More realistic calculations [28] within a model based on the hard thermal loop gluon propagator predict the value of hyperon polarization to be in the range from  $-0.03$  to  $0.15$  depending on the temperature of the QGP formed. Recent calculations [29,30] also explain the small value of the global  $\Lambda^0$  polarization observed at RHIC [23].

### 3. METHOD OF THE $\Lambda^0$ -POLARIZATION MEASUREMENT

The  $\Lambda^0$  hyperon has spin  $1/2$ . It decays to  $p + \pi^-$  with 64% branching ratio. The analysis of the angular distribution can be used to obtain the polarization value. The main method to measure  $\Lambda^0$  polarization in nucleus–nucleus collisions is the measurement of the emission angle distribution of the decay proton with respect to the system orbital momentum  $\mathbf{L}$ .

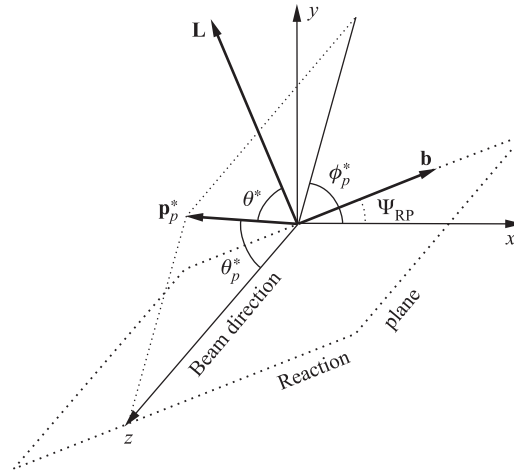


Fig. 2. The definition of the different angles for  $\Lambda^0$ -hyperon decay.  $x$ ,  $y$ ,  $z$  are the laboratory frame axes. The reaction plane is defined by the vectors of the initial beam  $\mathbf{z}$  and impact parameter  $\mathbf{b}$ .  $\mathbf{L}$  is the system orbital momentum normal to the reaction plane.  $\mathbf{p}^*$  and  $\theta^*$  are the proton three-momentum and the angle between the system orbital momentum  $\mathbf{L}$  and the three-momentum of the proton in the  $\Lambda^0$  rest frame, respectively.  $\Psi_{\text{RP}}$  is the reaction plane angle. The picture is taken from Ref. [23]

The definition of the different angles for  $\Lambda^0$ -hyperon decay is given in Fig. 2. Here  $x, y, z$  are the laboratory frame axes. The reaction plane is defined by the vectors of the initial beam direction  $z$  and impact parameter  $b$ .  $\mathbf{L}$  is the system orbital momentum normal to the reaction plane.  $\mathbf{p}^*$  and  $\theta^*$  are the proton three-momentum and the angle between the system orbital momentum  $\mathbf{L}$  and the three-momentum of the proton in the  $\Lambda^0$  rest frame, respectively.  $\Psi_{\text{RP}}$  is the reaction plane angle.

The decay proton distribution as a function of emission angle  $\theta^*$  is expressed as

$$\frac{dN}{d\cos\theta^*} = N_0(\cos\theta^*)(1 + \alpha\mathcal{P}_\Lambda \cos\theta^*), \quad (7)$$

where  $\mathcal{P}_\Lambda$  is the value of  $\Lambda^0$  polarization,  $\theta^*$  is the angle in the  $\Lambda^0$  rest frame between the system orbital momentum  $\mathbf{L}$  which is normal to the reaction plane and the decay proton,  $\alpha$  is an  $s$ - $p$ -wave interference term factor which is measured to be 0.642,  $N_0(\cos\theta^*)$  is the constant corrected for the geometry, efficiency, etc. The polarization is defined as the slope of the  $dN/d\cos\theta^*$  vs  $\cos\theta^*$ .

The global polarization of the hyperons measured at RHIC [23] is defined as the polarization  $\mathcal{P}_\Lambda$  averaged over the relative azimuthal angle

$$\mathcal{P}_\Lambda^G = \frac{3}{\alpha} \left\langle \cos\theta^* \right\rangle. \quad (8)$$

One can write global polarization in terms of the reaction plane angle  $\Psi_{\text{RP}}$  and the azimuthal angle  $\phi_p^*$  of the proton three-momentum in the  $\Lambda^0$  rest frame using the relation among the angles shown in Fig. 2 which is  $\cos\theta^* = \sin\theta_p^* \sin(\phi_p^* - \Psi_{\text{RP}})$  and integrating over the angle  $\theta_p^*$ :

$$\mathcal{P}_\Lambda^G = \frac{8}{\pi\alpha} \left\langle \sin(\phi_p^* - \Psi_{\text{RP}}) \right\rangle. \quad (9)$$

The expression (9) is similar to that used for the directed flow measurements.

#### 4. FEASIBILITY OF $\Lambda^0$ -POLARIZATION MEASUREMENT AT HIGH ENERGIES

From UrQMD transport model one can expect production of approximately  $20\Lambda^0$ 's decaying into  $p\pi^-$  pair in the central Au–Au collisions at 25 GeV · A.

The important feature of CBM setup [31] is quite large acceptance for the detection of the both protons and pions. Therefore, it is possible to detect the  $\Lambda^0$  hyperons with large transverse momenta  $p_T$ , where maximal effect in polarization properties is expected.

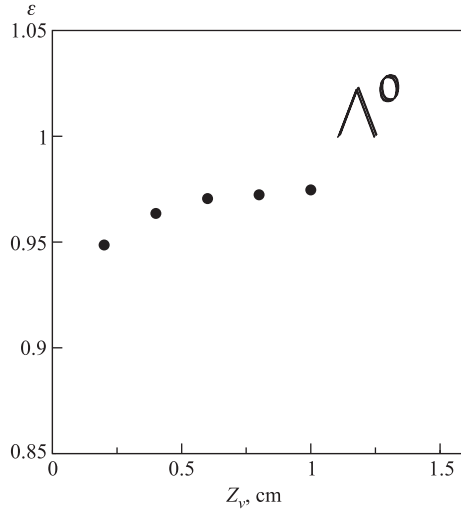


Fig. 3. The purity of  $\Lambda^0$ -hyperon selection with simple kinematical  $V^0$  fit as a function of the longitudinal secondary vertex position

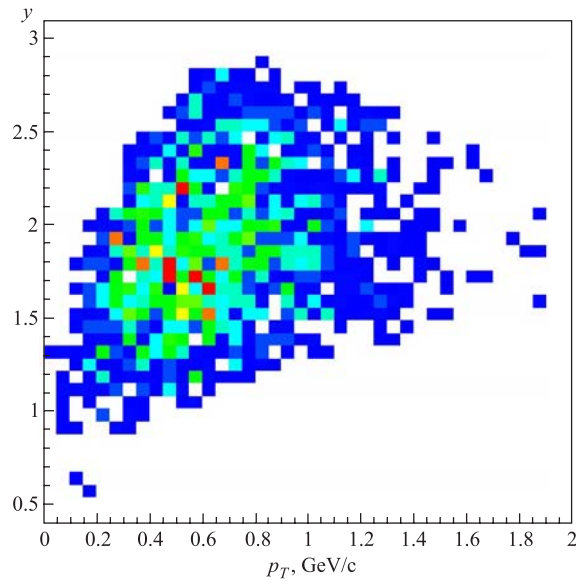


Fig. 4. The  $y$ - $p_T$  acceptance for reconstructed  $\Lambda^0$ 's from Au-Au central collisions at 25 GeV  $\cdot$  A for the conditions of CBM experiment



Silicon Tracking System (STS) consisting of seven or eight stations can provide the good tracking with the expected good enough efficiency. Since  $\Lambda^0$  is a weakly decaying particle ( $c\tau = 7.89$  cm), its decay vertex is well separated from the primary vertex. However, it is necessary to provide high efficiency of the secondary tracks finding. The selection of  $\Lambda^0$  hyperons at CBM can be done without the secondary particles identification to increase the acceptance. In this case the main source of the background is  $K_S^0$  meson decaying into  $\pi^+\pi^-$  pair.

The detailed feasibility study of the  $\Lambda^0$ -hyperon production at CBM [32] has been performed using track reconstruction based on the cellular automata method [31]. The mass and longitudinal secondary vertex resolutions achieved were  $M_\Lambda \sim 0.85$  MeV/ $c^2$  and 0.8 mm, respectively.

An alternative approach has been developed in Ref. [33]. Special  $V^0$ -particles ( $\Lambda^0$  and  $K_S^0$ ) finder has been developed using track reconstruction based on the conformal mapping and approximate solution of motion equation [34]. The precision of secondary vertex reconstruction was  $\sim 150$   $\mu\text{m}$  and  $\sim 100$   $\mu\text{m}$  for

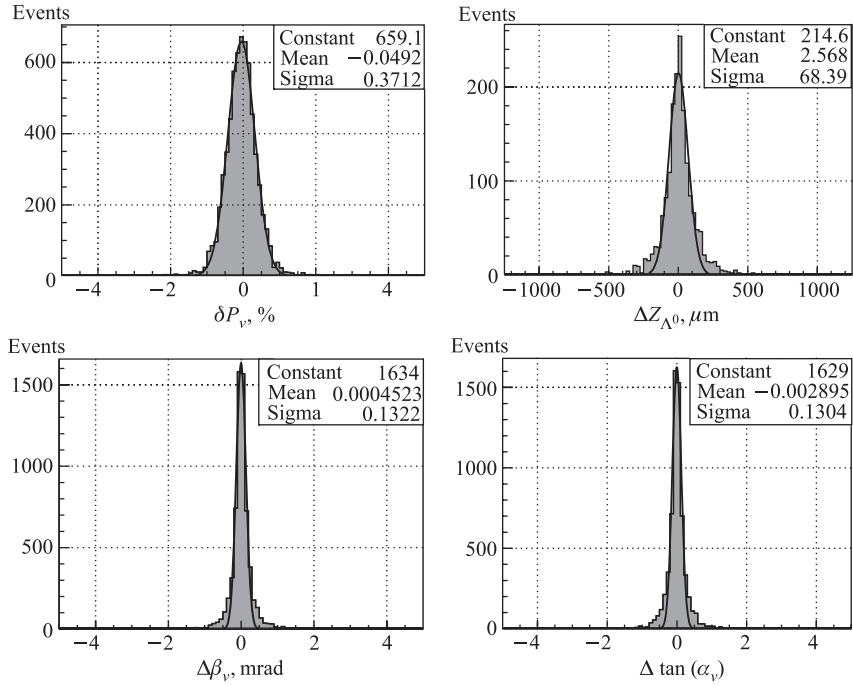


Fig. 5. The momentum, vertex position and angles reconstruction precisions for  $\Lambda^0$ 's from Au–Au central collisions at 25 GeV · A [33]

$\Lambda^0$  and  $K_S^0$ , respectively. The simple  $V^0$  fit used the energy and momentum conservation laws only:

$$\begin{aligned} E_{V^0} &= E^+ + E^- \\ \mathbf{p}_{V^0} &= \mathbf{p}^+ + \mathbf{p}^- \end{aligned} \quad (10)$$

with the fixed values of the  $V^0$ -particles masses. The purity of  $\Lambda^0$ -hyperon selection with simple  $V^0$  fit is shown in Fig. 3 as a function of the longitudinal vertex position. One can see that the purity of  $\Lambda^0$  selection is about 0.97 for the decay longitudinal vertex position larger than 5 mm.

The  $y$ - $p_T$  acceptance for reconstructed  $\Lambda^0$ 's from Au–Au central collisions at 25 GeV · A for the conditions of CBM experiment is shown in Fig. 4.

However, the measurement of the  $\Lambda^0$  polarization requires good knowledge of the kinematical parameters of the  $\Lambda^0$ , as well as the reaction plane and centrality value. The latest two parameters at CBM can be measured by zero degree calorimeter [35] with good precision. The  $V^0$  fitter [33] improves significantly the parameters of the  $\Lambda^0$  hyperons. The momentum and angular resolutions achieved are  $\delta p/p \sim 0.37\%$ ,  $\sigma_\beta \sim 0.13$  mrad and  $\sigma_{\tan \alpha} \sim 0.13$ , respectively. The precision of secondary vertex reconstruction was better than  $\sim 70 \mu\text{m}$ . The distributions on the reconstructed momentum, angles and vertex position for  $\Lambda^0$ 's are given in Fig. 5.

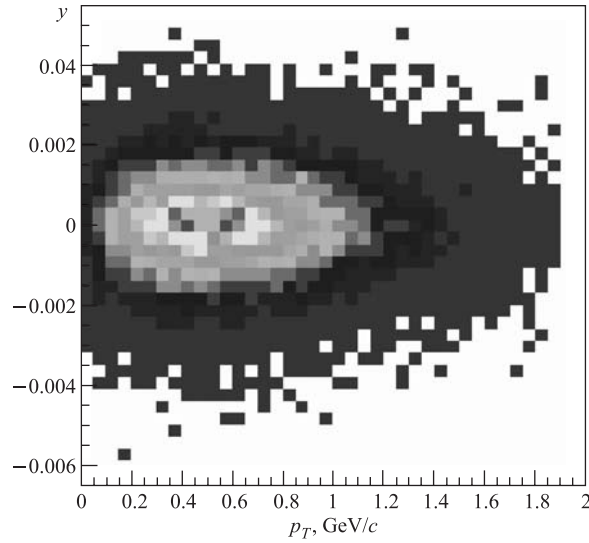


Fig. 6. The  $y$ - $p_T$  acceptance for  $\Lambda^0$ 's from Au–Au central collisions at  $\sqrt{s_{NN}} = 7.1$  GeV for the collider mode

The collider mode provides more symmetrical acceptance for  $\Lambda^0$  hyperons, that is significant for the proper reconstruction of the polarization. The  $y-p_T$  ideal acceptance for  $\Lambda^0$ 's from Au–Au central collisions at  $\sqrt{s_{NN}} = 7.1$  GeV for the collider mode (assuming the axial symmetry of MPD [36]) is shown in Fig. 6. Since no particle identification is required, the transverse momenta  $p_T$  achieved can be large enough to measure sizable polarization effects for  $\Lambda^0$  production. The reaction plane and impact parameter at MPD [36] can be measured with zero degree calorimeter assumed to be the same as at CBM setup or via charged particles energy flow reconstructed in the time-projection chamber.

## CONCLUSIONS

The measurement of the  $\Lambda^0$  polarization in nucleus–nucleus collisions at the energies of FAIR and NICA can be a new important tool in addition to the traditional ones to study the phase transition.

Feasibility of the  $\Lambda^0$  selection in Au–Au collisions at 25 GeV · A for the fixed target experiment is shown [31]. The study of the polarization effects in hyperon production for the collider mode [36] at the same energies has certain advantages and could be promising.

The authors thank Prof. A.I.Malakhov for the stimulating support of this work and O.V.Rogachevsky for the help in the simulation. This work has been supported in part by the Russian Foundation for Basic Research under grant No.07-02-00102a.

## REFERENCES

1. Panagiotou A. D. // Phys. Rev. C. 1986. V. 33. P. 1999.
2. Ayala A. et al. // Phys. Rev. C. 2002. V. 65. P. 024902.
3. Jacob M. // Z. Phys. C. 1988. V. 38. P. 273.
4. Herrera G., Magnin G., Montano L. M. // Eur. Phys. J. C. 2005. V. 39. P. 95.
5. Ioffe B. L., Kharzeev D. E. // Phys. Rev. C. 2003. V. 68. P. 061902(R).
6. Bratkovskaya E. L., Cassing W., Mosel U. // Z. Phys. C. 1997. V. 75. P. 119.
7. Liang Z.-T., Wang X.-N. // Phys. Rev. Lett. 2005. V. 94. P. 102301.
8. Liang Z.-T., Wang X.-N. // Phys. Lett. B. 2005. V. 629. P. 20.
9. Afanasiev S. V. et al. // Phys. Rev. C. 2002. V. 66. P. 054902.
10. Anticic T. et al. // Phys. Rev. Lett. 2004. V. 93. P. 022302.
11. Merschmeyer M. et al. // Phys. Rev. C. 2007. V. 76. P. 024906.
12. Justice M. et al. // Phys. Lett. B. 1998. V. 440. P. 12.
13. Albergo S. et al. // Phys. Rev. Lett. 2002. V. 88. P. 062301.

14. Barrette J. et al. // Phys. Rev. C. 2000. V. 63. P. 014902.
15. Adcox K. et al. // Phys. Rev. Lett. 2002. V. 89. P. 092302.
16. Adler C. et al. // Phys. Rev. Lett. 2002. V. 89. P. 092301.
17. Abelev B. I. et al. // Phys. Rev. Lett. 2006. V. 97. P. 132303.
18. Adams J. et al. // Phys. Rev. Lett. 2007. V. 98. P. 062301.
19. Abelev B. I. et al. // Phys. Rev. C. 2008. V. 77. P. 044908.
20. Harris J. et al. // Phys. Rev. Lett. 1981. V. 47. P. 229.
21. Anikina M. et al. // Z. Phys. C. 1984. V. 25. P. 1.
22. Bellwied R. et al. // Nucl. Phys. A. 2002. V. 698. P. 499c.
23. Abelev B. I. et al. // Phys. Rev. C. 2007. V. 76. P. 024915.
24. Lesnik A. et al. // Phys. Rev. Lett. 1975. V. 35. P. 770.
25. Bunce G. et al. // Phys. Rev. Lett. 1976. V. 36. P. 1113.
26. Heller K. et al. // Phys. Lett. B. 1977. V. 68. P. 480; Phys. Rev. Lett. 1978. V. 41. P. 607; Phys. Rev. Lett. 1983. V. 51. P. 2025;  
Abe F. et al. // Phys. Rev. Lett. 1983. V. 50. P. 1102; Phys. Rev. D. 1986. V. 34. P. 1950;  
Bonner B. E. et al. // Phys. Rev. D. 1988. V. 38. P. 729;  
Smith A. M. et al. // Phys. Lett. B. 1987. V. 185. P. 209;  
Lundberg B. et al. // Phys. Rev. D. 1989. V. 40. P. 3557;  
Henkes T. et al. // Phys. Lett. B. 1992. V. 283. P. 152;  
Ramberg E. J. et al. // Phys. Lett. B. 1994. V. 338. P. 403;  
Fanti V. et al. // Eur. Phys. J. C. 1999. V. 6. P. 265;  
Alev A. N. et al. // Eur. Phys. J. C. 2000. V. 13. P. 427.
27. DeGrand T. A., Miettinen H. I. // Phys. Rev. D. 1981. V. 23. P. 1227; Phys. Rev. D. 1981. V. 24. P. 2419; Phys. Rev. D. 1985. V. 31. P. 661(E);  
DeGrand T. A., Markkanen J., Miettinen H. I. // Phys. Rev. D. 1985. V. 32. P. 2445.
28. Liang Z.-T. // J. Phys. G: Nucl. Part. Phys. 2007. V. 34. P. S323.
29. Gao J.-H. et al. // Phys. Rev. C. 2008. V. 77. P. 044902.
30. Barros C. C., Jr., Hama Y. arXiv:0712.3447 [hep-ph].
31. Senger P. // Nucl. Phys. A. 2008. V. 804. P. 274.
32. Kryshen E., Berdnikov Y. CBM-PHYS-note-2005-002. 2005.
33. Jerusalimov A. P. JINR Preprint E10-2009-171. Dubna, 2009; submitted to «Part. Nucl., Lett.».
34. Jerusalimov A. P. JINR Preprint E10-2009-157. Dubna, 2009; submitted to «Part. Nucl., Lett.».
35. Guber F. et al. CBM-PSD-note-2006-001. 2006.
36. Sissakian A. N., Sorin A. S. (for NICA Collab.) // J. Phys. G. 2009. V. 36. P. 064069.

Received on December 3, 2009.

Редактор *Е. И. Кравченко*

Подписано в печать 18.03.2010.

Формат 60 × 90/16. Бумага офсетная. Печать офсетная.

Усл. печ. л. 0,81. Уч.-изд. л. 1,11. Тираж 365 экз. Заказ № 56932.

Издательский отдел Объединенного института ядерных исследований  
141980, г. Дубна, Московская обл., ул. Жолио-Кюри, 6.

E-mail: [publish@jinr.ru](mailto:publish@jinr.ru)

[www.jinr.ru/publish/](http://www.jinr.ru/publish/)